Radiative Transfer and Applications to Very Large Telescopes
Ph. Stee (ed)
EAS Publications Series, **18** *(2006) 129–155*

INCLUDING ALL THE LINES

R.L. Kurucz[1]

Abstract. We present a progress report on including all the lines in the linelists, including all the lines in the opacities, including all the lines in the model atmosphere and spectrum synthesis calculations, producing high-resolution, high-signal-to-noise atlases that show (not quite) all the lines, so that finally we can determine the properties of stars from a few of the lines.

1 Atomic and Molecular Line Data

Of the line data on my website, 99 percent have predicted wavelengths and can be used only to compute opacities. One percent have good wavelengths between known levels and can be used for detailed spectrum calculations for comparision to observed spectra. The line data with good wavelengths account for only one half of the observed lines. The *gf* values and damping constants for most lines must be adjusted to match observed spectra. We know that the higher configurations are missing from the line lists. We know that heavier elements are missing from the line lists. We know that isotopic and hyperfine splittings are missing from the line lists. We know that many molecules are missing from the line lists. Leaving out all these lines systematically underestimates the opacity, produces energy distributions with systematic errors, and leads to abundance determinations with large systematic errors. The most sophisticated 3-D radiation-hydrodynamics calculations for stars are still wrong if the opacities are wrong.

We need much better laboratory analyses including hyperfine and isotopic splitting. We need better calculations that fill in the higher configurations and the heavier elements. We need better measurements and calculations for all the significant diatomic and polyatomic molecules including all the isotopomers.

I am doing as much as I can to fill in the missing data and to make it available on my web site.

Half the lines in the solar spectrum are not identified. All the features are blended. Most features have unidentified components that make it difficult to

[1] Harvard-Smithsonian Center for Astrophysics, 60 Garden Street, Cambridge, MA, USA
e-mail: rkurucz@cfa.harvard.edu

© EAS, EDP Sciences 2006
DOI: 10.1051/eas:2006009

Article published by EDP Sciences and available at http://www.edpsciences.org/eas or http://dx.doi.org/10.1051/eas:2006009

treat any of the identified components in the blend. And even the known lines have hyperfine and isotopic splittings that have not yet been measured. Is an asymmetry produced by a splitting, or by a velocity field, or both? It is very difficult to determine abundances, or any property, reliably when you do not know what you are working with. Figure 1 illustrates these points. It shows one of the emptiest angstroms in the visible in a high-resolution, high-signal-to-noise solar spectrum taken by James Brault with the FTS at Kitt Peak together with the spectrum calculated with SYNTHE. Figure 2 is a sample section of the spectrum of Sirius observed by Glenn Wahlgren with the Goddard High Resolution Spectrograph on the Space Telescope together with the calculated spectrum.

[Fig. 1 is a large color ledger page on the Kurucz website `KURUCZ.HARVARD.EDU/PAPERS/NICELINES/FIG1`. It will be mailed by post on request.]

Fig. 1. A small section of the solar flux spectrum at 599 nm plotted at full scale and at 10-times scale. The heavy black lines show the observed spectrum from the Kitt Peak Solar Flux Atlas from 300 to 1000 nm (Kurucz 2005). The resolving power is about 300 000 and the signal-to-noise is about 3000. Higher quality spectra would be helpful because the spectrum is not resolved and because weaker features would appear at higher signal-to-noise.

The thin lines are the computed spectra: in red for the solar flux, in blue for the telluric atmospheric transmission, and in purple for their product which should be compared to the observed heavy black lines. The computed spectra are broadened to resolving power 0.05666 cm^{-1} to match the observed spectrum. There are solar lines of Ca I, Ti I, Cr I, Cr II, Fe I, Fe II, Co I, Yb II, C_2, CN, and telluric lines of H_2O. The first number in each line label is the last 3 digits of the wavelength. The second number is the species code which is the atomic number plus 0.01 times the charge. The middle numbers are either the lower energy level in cm^{-1} for atoms or quantum numbers for molecules. The 4th number is the per mil line depth if the line were computed in isolation. Two of the Co I lines have been divided into hyperfine components. The hyperfine and isotopic splittings have not yet been determined for the other lines. Some splittings may be negligible. There are many missing lines. The lines that are present have been adjusted to improve agreement between the calculated and observed spectra. That process is continuing. This sample will be part of a forthcoming flux atlas with line identifications.

[Fig. 2 is a large color ledger page on the Kurucz website `KURUCZ.HARVARD.EDU/PAPERS/NICELINES/FIG2`. It will be mailed by post on request.]

Fig. 2. A sample section of the spectrum of Sirius at 200 nm observed by Glenn Wahlgren with the Goddard High Resolution Spectrograph on the Space Telescope together with a calculated spectrum that has not yet been adjusted to improve the fit.

The rotation velocity is known from fitting lines in the visible observed at high resolution. The spectrum is computed both at 0 $km\,s^{-1}$ rotation velocity to resolve the blends and at 16 $km\,s^{-1}$. The 16 $km\,s^{-1}$ spectrum was then convolved with the instrumental profile. The resolution was not high enough to resolve the

actual structure in the spectrum which is on the order of the zero rotation line width. Around 201.26 for example the two side bumps are washed out. Ideally the measurement should have been made at higher resolution.

The calculations are plotted in residual flux but the continuum level for the observed spectrum has not been set and its position can be adjusted. Except at 201.02 nm it appears that the observed spectrum should be moved up about 3%. That would also bring the minima into better agreement. Either the Mn II line at 201.0259 is wrong or there is a problem with the reduction at this point which is near the end of a scan. Note that the minima in the spectrum at 201.1, 201.22, and 201.42 are not line positions. Features in spectrum are blends of many lines.

Note the Si II line at 201.5 that is computed very much too strong. That will be corrected in my next calculation for Si II. Note the missing line at 201.11. That will probably appear when I recompute the Fe group lines using improved laboratory analyses. The linelist for this spectrum has not been updated with new calculations. It uses the linelist from my web site. I am going to update many elements at once to limit the number of versions of the linelist and also to give me more time to make comparisons and to check for errors. Fresh calculations can be found on the website in the /ATOMS directory.

For planetary and telluric atmosphere projects the solar irradiance spectrum is required as the input at the top of the atmosphere. It has never been observed. People ask me to compute it. I can compute it theoretically using both known and predicted lines and get agreement averaged over a nanometer but there is no way to predict the resolved spectrum when only half the lines are known. In other stars the situation is worse because the signal-to-noise and resolution of the observations are worse. Logically one has to know *a priori* what is in the spectrum in order to interpret it; there is not enough information in the observed spectrum itself.

Basically we need a list of all the energy levels of all atoms and molecules that matter (qualifiers below). From that list can be generated all the lines. With the energy levels and line positions known, one can measure *gf* values, lifetimes, damping, or one can determine a theoretical or semiempirical Hamiltonian whose eigenvalues and eigenvectors produce a good match to the observed data, and that can then be used to generate additional radiative and collisional data for atoms or molecules. Forbidden magnetic dipole and electric quadrupole lines are required as well.

For atoms and ions, we need all levels, including hyperfine and isotopic splittings, for $n \leq 9$ below the lowest ionization limit and as much as practicable above. Lifetimes and damping constants depend on sums over the levels.

Radiative acceleration in stellar envelopes can selectively levitate some elements. At the visible surface the enhancement can be as much as a factor of 10^4. The radiative acceleration is computed by integrating $l_\nu J_\nu$ over the spectrum. If the diffusion takes place deep in the envelope, spectra for high stages of ionization are required. For heavier elements we need at least the first 5 stages of ionization.

In the sun I see unidentified asymmetric triangular features that are unresolved multiplets of light elements with $n \leq 20$. Simple spectra should be analyzed up

to $n = 20$. Levels that connect to the ground or to low levels should be measured to high n, say $n = 80$. The high levels are necessary to match line series merging into continua.

For molecules, we need all levels below the first dissociation limit and as much as is practicable above, especially levels of all states that connect to the ground state. Except for H_2(BX,CX), far ultraviolet bands have been ignored unless they appear as interstellar lines. We see H_2 lines in stars as hot as 8000 K when the stars have low metal abundances so that the lines are not masked.

In the sun we see, and have line lists for, C_2(AX, ba, da, ea), CN(AX, BX), CO(AX, XX), H_2(BX, CX), CH(AX, BX, CX), NH(AX, ca), OH(AX, XX), MgH(AX, BX), SiH(AX), SiO(AX, EX, XX). The isotopomers are included. Some stellar spectroscopists have more recent linelists than I do. Mine are based on old laboratory data and were computed with rotationless RKR potentials. They all have to be brought up to date, or even further improved, and expanded to higher V and J levels. In many cases there are new analyses based on FTS spectra. Ions and a few minor molecules have to be added to the linelist as well. In the sun there are many broad bumpy unidentified features that are molecular bands that are not in the line lists. Most of them are probably just high-V transitions. It is important that the laboratory analyses include all the isotopomers. They are needed to interpret the stellar spectra. When they are not measured in the laboratory, we have to make up our own predicted linelists for them.

For the cooler stars we need all the diatomics among all the abundant elements, and, essentially, the hydrides and oxides for all elements (such as ScO. TiO, VO, YO, ZrO, LaO, etc.). Ca appears as CaOH and CaH, not CaO. I use the TiO linelist from Schwenke (1998) with 38 million lines.

Stars that are evolved and have high C abundances from nuclear burning can bind all the O into CO so that there are no other oxides, just C-bearing molecules. CN and C_2 bands are everywhere.

For M stars cooler than 3500 K triatomics also become important. Much more laboratory and computational work is needed for H_2O. I currently use the linelist from Partridge and Schwenke (1997) with 66 million lines.

In the brown dwarfs and "planets" methane is important and it needs more laboratory and computational work.

Some of this is described in more detail in my paper "Atomic and molecular data needs for astrophysics" (Kurucz 2002).

1.1 Isotopic and Hyperfine Splitting

There are two papers on isotopic and hyperfine splitting on my website (Kurucz 1992, 1993). In the second is a table that lists all the stable isotopes, their fractional abundances, nuclear spin, dipole moment, and quadrupole moment. The only element that does not have isotopic or hyperfine splitting is thorium. "Lines" are normally asymmetric because of the splitting. Figure 3 from Rosberg *et al.* (1992) show the isotopic splitting of an Fe II line and a Ni II line. If the splitting is not taken into account many kinds of errors are possible: the use of bisectors to

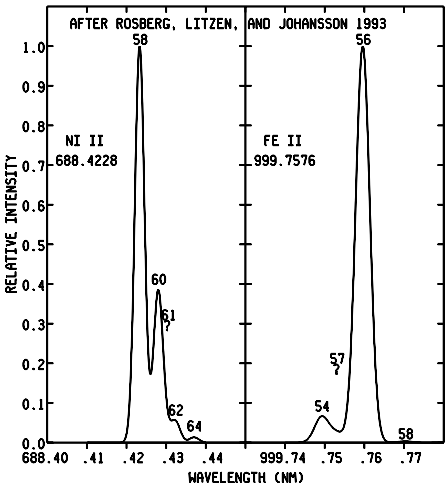

Fig. 3. Examples of isotopic splitting in Fe II and Ni II after Rosberg *et al.* (1993). The indications for ^{61}Ni and ^{57}Fe are guesses.

determine velocity fields is incorrect; Fourier analysis of line profiles to determine rotational, microturbulent, and macroturbulent velocities is incorrect; damping constants are over-estimated. When stronger components become saturated, the weak components are still on the linear part of the curve of growth. They make a larger contribution to the total feature than their fractional abundances might suggest. This introduces the additional systematic errors: wavelengths of saturated lines are shifted relative to the isotopic abundance weighted position; abundances determined from equivalent widths are wrong unless the curve of growth is computed from the real line profile with components. In addition, the Doppler width and Voigt profile differ significantly from the lightest to the heaviest isotope.

I was recently asked about the Ca II infrared triplet so I collected the data from the literature. Figure 4 shows the solar flux spectra for the cores of the Ca II infrared triplet lines for two Å around their centroid wavelengths and with the LTE computed profiles including hyperfine and isotopic splitting. In non-LTE the cores become weaker as observed. The components are listed in Table 1.

Molecular lines can also have hyperfine splitting, but I have not yet had to deal with it.

1.2 Adding Atomic and Molecular Data

The basic rule seems to be that if you need data you have to produce it yourself. My workstation and my website have a directory for each ion of all the atoms up through Zn, and the first five ions of heavier elements, and for all the diatomic molecules that I should work on. Here are a few examples:

Fe II. The semiempirical calculation for $n \leq 9$ was based on Johansson (1978) and on more recent published and unpublished data. Johansson has data for more

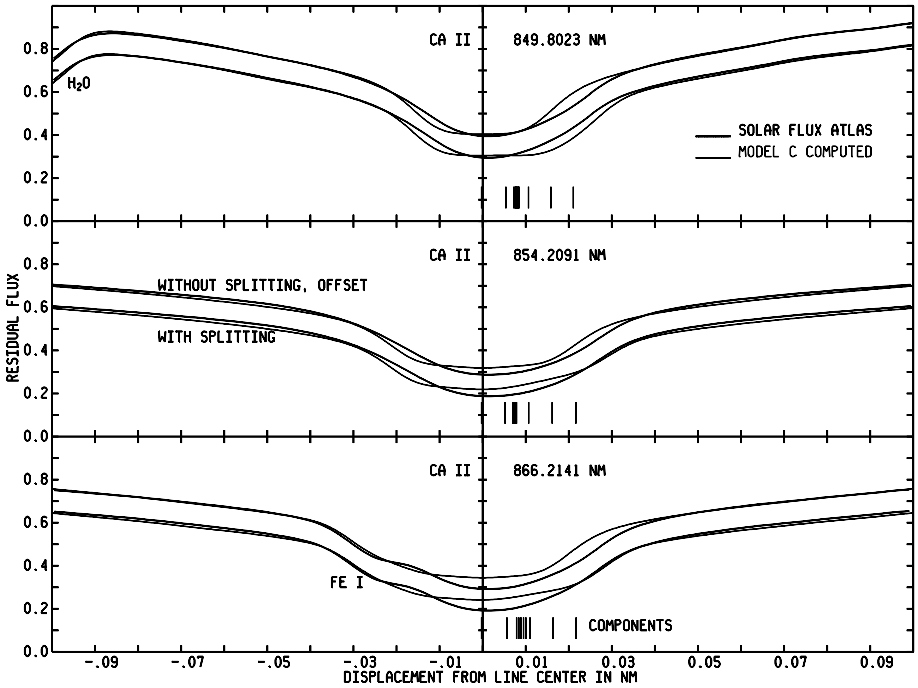

Fig. 4. Asymmetries in the Ca II infrared triplet arise from isotopic and hyperfine splittings, not from velocity or non-LTE effects. The splitting data are listed in Table 1. Two Å around each line are plotted twice, centered on the centroid wavelength, with splitting, and, offset, without splitting. The calculation uses model C by Fontenla *et al.* (1993) which has a chromosphere. In lieu of a real non-LTE calculation, the line opacity was smoothly changed to scattering for $\tau_{\rm Ross} < 0.04$. The number was chosen by experimenting until the emission from the chromosphere was eliminated. Note that the splitting also changes the line wings. The heavy lines are the observed spectrum from the Kitt Peak Solar Flux Atlas from 300 to 1000 nm (Kurucz 2005).

than 100 energy levels that I do not yet have. There were 46 even configurations: d^7, d^6ns, nd, ng, ni, nl, d^54sns, nd, ng, ni, nl, d^44s^24d, d^44s^25s, d^54p^2 which produce 19 771 levels of which 403 are known. There are 39 odd configurations: d^6np, nf, nh, nk, d^54snp, nf, nh, nk, d^44s^24p, d^44s^25p, d^54s^24f, which produce 19 652 levels of which 492 are known. These produced 7 719 963 E1 lines and 28 million M1 and E2 lines. Only 81 225 E1 lines have good wavelengths. Only 2884 of the forbidden lines are from metastable levels. The previous calculation (Kurucz 1988) produced 1 264 969 lines with 45 815 good wavelengths. There are four stable isotopes:

Isotopes	^{54}Fe	^{56}Fe	^{57}Fe	^{58}Fe
Fraction	.059	.9172	.021	.0028

Table 1. Hyperfine and isotopic splitting for the Ca II infrared triplet.

Centroid data from KURUCZ.HARVARD.EDU/LINELISTS/GFALL/GF2001.ALL

wl(nm)	loggf	ref	E	J	label	E'	J'	label'	gamr	gams	gamw	glande	glande'
849.8023	-1.312	BWL	13650.190	1.5	3d 2D	25414.400	1.5	4p 2P	8.20	-5.55	-7.80	0.800	1.334
854.2091	-0.362	BWL	13710.880	2.5	3d 2D	25414.400	1.5	4p 2P	8.20	-5.55	-7.80	1.200	1.334
866.2141	-0.623	BWL	13650.190	1.5	3d 2D	25191.510	0.5	4p 2P	8.19	-5.55	-7.80	0.800	0.666

Hyperfine A and B for 43Ca II, spin I 3.5

E	J	label	A(MHz)	B(MHz)	ref
0.000	0.5	4s 2S	-797.5	0.0	GM
13650.190	1.5	3d 2D	-52.	-4.42	MPS
13710.880	2.5	3d 2D	-5.2	-6.305	MPS
25191.510	0.5	4p 2P	-158.0	0.0	GM
25414.400	1.5	4p 2P	-30.9	-10.1	MPS

Isotopic splitting from MP (46 and 48 extrapolated)

wl(nm)	iso	log hyper f	log iso frac	F	F'	hfshift dE(mK)	isoshift dE' (mA)	wl(nm)	iso	log hyper f	log iso frac	F	F'	hfshift dE(mK)	isoshift dE' (mA)
849.8020	40	0.000	-0.013			0	0 -3	866.2138	40	0.000	-0.013			0	0 -3
849.8077	42	0.000	-2.189			0	0 +54	866.2197	42	0.000	-2.189			0	0 +54
849.8095	43	-1.017	-2.870	5-4	-9	0	+78	866.2220	43	-0.931	-2.870	4-3		0	12 +78
849.8098	43	-0.903	-2.870	4-3		0	4 +78	866.2225	43	-0.785	-2.870	3-3		7	12 +78
849.8099	43	-0.606	-2.870	5-5	-9	-5	+78	866.2229	43	-0.806	-2.870	2-3		12	12 +78
849.8101	43	-1.028	-2.870	3-2		7	7 +78	866.2229	43	-0.464	-2.870	5-4		-9	-9 +78
849.8101	43	-1.222	-2.870	4-4		0	0 +78	866.2236	43	-0.785	-2.870	4-4		0	-9 +78
849.8105	43	-1.204	-2.870	2-2		12	7 +78	866.2241	43	-1.262	-2.870	3-4		7	-9 +78
849.8105	43	-1.017	-2.870	4-5		0	-5 +78	866.2251	44	0.000	-1.681			0	0 +109
849.8106	43	-0.903	-2.870	3-4		7	0 +78	866.2304	46	0.000	-4.398			0	0 +163
849.8107	43	-1.028	-2.870	2-3		12	4 +78	866.2358	48	0.000	-2.728			0	0 +217
849.8129	44	0.000	-1.681			0	0 +109								
849.8181	46	0.000	-4.398			0	0 +161								
849.8233	48	0.000	-2.728			0	0 +213								
854.2088	40	0.000	-0.013			0	0 -3								
854.2143	42	0.000	-2.189			0	0 +52								
854.2161	43	-1.204	-2.870	2-2		2	7 +74								
854.2161	43	-1.505	-2.870	3-2		1	7 +74								
854.2162	43	-1.204	-2.870	1-2		2	7 +74								
854.2163	43	-1.380	-2.870	2-3		2	4 +74								
854.2163	43	-1.040	-2.870	3-3		1	4 +74								
854.2163	43	-1.066	-2.870	4-3		0	4 +74								
854.2165	43	-0.783	-2.870	5-4		0	0 +74								
854.2166	43	-1.630	-2.870	3-4		1	0 +74								
854.2166	43	-1.032	-2.870	4-4		0	0 +74								
854.2168	43	-0.567	-2.870	6-5	-2	-5	+74								
854.2169	43	-2.058	-2.870	4-5		0	-5 +74								
854.2169	43	-1.193	-2.870	5-5		0	-5 +74								
854.2198	44	0.000	-1.681			0	0 +107								
854.2252	46	0.000	-4.398			0	0 +161								
854.2307	48	0.000	-2.728			0	0 +216								

GM Goble, A.T. and Maleki, S. 1990, Phys. Rev. A 42, 649-650.

MPS Martensson-Pendrill, A. and Salomonson, S. 1984. Phys. Rev. A 30, 712-721.

MP Martensson-Pendrill,A-M., Ynnerman, A., et al. 1992. Phys. Rev. A 45, 4675-4681.

Only a few lines have been measured by Rosberg *et al.* (1993) so I put in the splittings by hand.

The **Ni I** calculation was mostly based on the analysis by Litzén *et al.* (1993) which includes isotopic splitting. There were 46 even configuations with 3203 levels of which 120 are known. There were 48 odd configurations with 4800 levels of which 153 are known. These produced 529 632 E1 lines compared to 149 926 from Kurucz (1988). Only 9637 lines have good wavelengths. There were 1.5 million M1 and E2 lines of which 65 were from metastable levels. There are 5 stable isotopes,

Isotope	^{58}Ni	^{60}Ni	^{61}Ni	^{62}Ni	^{64}Ni
Fraction	.6827	.2790	.0113	.0359	.0091

There are measured splittings for 326 lines from which I determined 131 energy levels relative to the ground. These levels are connected by 11 670 isotopic lines. Hyperfine splitting was included for ^{61}Ni but only 6 levels have been measured which produce 4 lines with 38 components. A pure isotope analysis is needed.

Ni I lines are asymmetric from the splitting. When the isotopic calculation was first checked against the solar spectrum it did not look right. Subsequently, I found a program error and recomputed the splittings. Now the profiles match the observed. Observed stellar spectra are generally not high enough quality to show that there are such errors.

The **Co I** calculation was based on Pickering & Thorne (1996) and on Pickering (1996) with hyperfine splitting. This calculation was made before my programs were expanded. I will rerun this with twice as many configurations. This calculation had 32 even configurations with 3546 levels of which 139 were known. There were 32 odd configurations with 5870 levels of which 223 were known. These produced 1 729 299 E1 lines of which 15 481 were between known levels. The old calculation (Kurucz 1988) produced 54 6130 lines. There were 4.7 million forbidden lines of which 696 were from metastable levels, ^{59}Co is the only stable isotope. Hyperfine constants have been measured in 297 levels which produce 244 264 component E1 lines. I have not yet computed the M1 or E2 components. The new calculation greatly improves the appearance of the Co I lines in the solar spectrum.

C I. The lower levels of C I were computed as in the previous examples and higher levels up to $n = 20$ were added from Ritz extrapolation for low l or from the polarization formula for high l. There were 136 even configurations: s^2p^2, s^2pnp, nf, nh, nk, nm, no, nr, nv, nw, ny, with 2382 levels. There were 139 odd configurations: s^2pns, nd, ng, ni, nl, nn, nq, nt, nv, nx, sp^2np, p^3ns, p^3nd, with 1962 levels. They produced 469 918 E1 lines of which 182 979 have good wavelengths. The low levels produced 652 897 forbidden lines of which 10 were from metastable levels. The series were extrapolated to $n = 99$ to produce 36 182 lines that merge into low continua. I have not yet worked on the isotopic or hyperfine splitting. The isotopes are 0.9890 ^{12}C and 0.0110 ^{13}C.

I am now doing Si I in the same way.

S I. There were 61 even configuarations with 2161 levels and 61 odd configuartions with 2270 levels. They produced 225 605 E1 lines of which 24 722 had good wavelengths. I have added measured autoionization parameters to the ultraviolet lines by hand. There are 4 stable isotopes,

Isotopes	^{32}S	^{33}S	^{34}S	^{36}S
Fraction	.9502	.0075	.0421	.0002

I have not yet worked on the isotopic or hyperfine splitting.

TiO. Schwenke (1998) calculated energy levels for TiO including in the Hamiltonian the 20 lowest vibration states of the 13 lowest electronic states of TiO (singlets a, b, c, d, f, g, h and triplets X, A, B, C, D, E) and their interactions. He determined parameters by fitting the observed energies or by computing theoretical values. Using Langhoff's (1998) transition moments Schwenke generated

a linelist for $J = 0$ to 300 for the

Isotopomers	^{46}TiO	^{47}TiO	^{48}TiO	^{49}TiO	^{50}TiO
Fraction	.080	.073	.738	.055	.054

My version has 37 744 499 lines.

Oxides. Good laboratory analyses and a semiempirical treatment similar to that for TiO are needed for CaOH, ScO, VO, YO, ZrO, LaO, etc. Better laboratory data could be used to further improve TiO.

2 Rapid Computation of Line Opacity in SYNTHE and DFSYNTHE

Once we have the line data we need to compute opacities. There is a paper on my website, "Rapid Calculation of Line Opacity", `KURUCZ.HARVARD.EDU/PAPERS/OPACITYCALC`, that was never published, like many of my papers. It starts with a naive calculation and shows how to speed it up by a factor of 1000. Consult that for details. Here I will just mention some of the points.

There is no limit to the number of lines. I expect to reach more than one billion lines in the near future.

Do not compute to higher precision than the physics warrants. Wavelengths are the only physically accurate numbers in the whole problem. For everything else, 0.1 percent ($1/2^{10}$) is more than adequate. Very few *gf* values are accurate to 1 percent or even 10 percent. The lower energy that goes into the Boltzman factor needs only 0.1 percent accuracy. Damping constants are accurate from 1 to 100 percent. Abundances are accurate from 1 to 100 percent. Use a low precision Voigt function. Use two-byte integers. Never compute anything twice. Factor out T dependences and do all pressures together for a given T.

Once you have a program like SYNTHE, take a model (a T-P table), a linelist, and the program and compute the opacity spectrum from the far ultraviolet to the far infrared for 0 $V_{\rm turb}$. You then have an array of say 4 million points at 20 pressures at 50 temperatures. To include microturbulent velocity for, say, five values, either broaden the spectrum with a gaussian filter or Fourier transform the spectrum, broaden the transform, and transform back. Write out the log of the spectrum packed as two byte integers. Repeat for all the $V_{\rm turb}$ values. Do it over and over again for a range of temperatures and pressures.

Transpose the array to 20 pressures at 50 temperatures at 5 $V_{\rm turbs}$ at 4 million points. You can then generate a spectrum for a given model by interpolating in the table and integrating to get the flux. The table is 40 GB. This method may actually be practical with a large amount of disk space and a fast computer. You could add in the continuous opacity and store the total absorption and the total scattering in 80 GB. The model atmosphere program would not have to compute any opacities; it would just interpolate in the tables.

You can tabulate only a limited temperature, pressure, and wavelength range, say with no molecules and no far infrared, or with no multiple ions and no Lyman continuum, to save space and time. You can compute the opacities over only

limited wavelength regions, a photometric system, a single echelle order, a velocity template, and then recover the opacities by interpolation from a small table.

You can leave out the big lines so that you can treat them separately. You can leave out hydrogen lines so you can treat H_α or H_β separately. You can leave out all the lines of one element. You can include only the lines of one element. If you have very large storage you can tabulate the opacity spectrum of each element separately and add them together weighted by their abundances. (But without molecules, and there may be problems with broadening.)

If you have only a workstation and less disk space, you need to start making approximations. Instead of writing out a spectrum for a given P, T, $V_{\rm turb}$ you can statistically analyze it in wavelength intervals and represent thousands of points in an interval with only a small number of coefficients. A distribution function tells you the fraction of the interval occupied by high, medium, and low opacity (actually in 12 steps in DFSYNTHE). The distribution function approximation is valid if the shape of the spectrum is similar at different temperatures and pressures, *i.e.*, the maxima and minima line up, and if the source function does not vary strongly across the wavelength interval.

Fiorella Castelli in Trieste is the expert on using DFSYNTHE. She has recomputed most of my old ODFs using updated opacities including the new H_2O and TiO linelists. She is also the expert on using the ODFs to compute new grids of ATLAS9 models (Castelli & Kurucz 2003).

Each spectrum can be processed more than once, say with different size wavelength intervals. You can purposefully select wavelength intervals that have various sizes and follow features, or make distribution functions for whole continua to try to minimize the number of points.

There are other procedures for processing the opacity spectra. You can make opacity sampling tables by saving only every one hundredth point, leaving 40 000 points in only 400 MB, which would fit on a CD and even in memory on some computers. Then ATLAS12 could run without line data or opacity routines, just interpolations. Once you have pretabulated the opacity, you can pretabulate the Rosseland mean. With pretabulated Rosseland opacity ATLAS12 would converge much faster. Of course, ATLAS12 would lose the ability to change abundances.

You can purposefully select the wavelengths that are saved, or the wavelength intervals, or make selective means, or intermix different strategies. Instead of doing opacity sampling that maintains the dynamic range in the opacity, you can throw away the dynamic range and use mean opacities. Instead of sampling at every hundredth point, average every hundred points (inversely or in the log). This would work in ATLAS12 and would result in a mean fluxes at resolving power 5000. The fluxes would not be physically correct, but they can be checked by computing the spectrum point by point and averaging. It may be no worse than other shoddy physics, such as mixing-length convection, in the model atmosphere programs.

3 ATLAS12, SYNTHE, ATLAS9, WIDTH9, etc.

Once programs had been developed to compute a realistic opacity spectrum for large numbers of lines (SYNTHE, Kurucz & Avrett 1981) it became possible consider including all the lines in a model atmosphere calculation. I can do this directly but it would take about a month per model with the fastest Alpha workstation, and perhaps a day using the full power of a parallel supercomputer. More practical methods involve statistical treatments of the line opacity. I have programmed two different treatments. First, opacity distribution functions, ODFs, using DFSYNTHE to pretabulate the opacity, then ATLAS9 to compute the models and low resolution emergent flux, and finally SYNTHE and SPECTR to generate the high-resolution spectrum. Second, opacity sampling using ATLAS12 to compute both the opacity at a small number of points (30 000) and a model that conserves energy but does not produce accurate fluxes. Then SYNTHE and SPECTR are used to generate the emergent high-resolution spectrum.

SYNTHE and SPECTR can also generate specific intensity spectra across the disk that ROTATE uses to produce rotationally broadened flux spectra. The intensity spectra themselves are the limbdarkening. Spectra can be transmitted through the terrestrial atmosphere using the TRANSYNTHE suite of programs. The spectra can be convolved with filters to generate any color system using INTEGRATEFILTER. The spectra can be convolved with instrumental bandpasees to generate energy distributions, SEDs, or spectra at any resolution using BROADEN. The final computed spectra can be plotted together with the observed spectra with the lines labelled using PLOTSYN.

With a fast, large-memory workstation it is now possible to compute, for a fixed set of abundances, tables of ODF opacities in one day, and then to compute a whole grid of models in another day. A small section of spectrum, enough to calibrate a photometric system, or echelle orders, can be computed in another day for the whole grid of hundreds of models.

Alternatively, to work on individual stars with arbitrary abundances, including isotopic abundances, one can use ATLAS12 to generate in one day a small grid for one star that varies temperature, gravity, and abundances. In another day a small region of the spectram can be computed for each model and compared to observation. The whole spectrum can be computed for the best fitting model.

3.1 ATLAS12

ATLAS12 still does not work as originally advertised (Kurucz 1995). It is supposed to be able to treat abitrary abundances, including depth-dependent isotopic abundances. At that time I had become interested in isotopes; I had isotopomeric molecular line lists that could show variation from dredge-ups, and also I was interested in isotopic splittings of atomic lines and diffusion. There were two problems, treating Rosseland opacities and treating the equation of state, that had to be solved to get ATLAS12 to work. All of my model atmosphere programs except the first few use a Rosseland opacity scale. This is the "natural" scale for coupling the

structure of the atmosphere to the radiation field. Convective flux also depends on the Rosseland opacity. But for arbitrary, and espcially for depth-dependent abundances, the Rosseland opacity cannot be pretabulated. It has to be computed as the model is computed. It took me years to figure out how to generate a starting guess for the Rosseland opacity and to extrapolate from iteration to iteration as the temperature was changing. The guessing procedure worked and allowed ATLAS12 models to converge. At that point I started to let others use the program. Later it was pointed out to me by Tsymbal (Tsymbal & Shulyak 2003) that I could have chosen a continuum monochromatic optical depth scale that behaves similarly to the Rosseland depth scale, and that I could have computed the models on that depth scale. At each iteration I could compute the Rosseland opacity and use it to compute the convection. Once the model converged I could interpolate it to the Rosseland scale. This should work except in cases where there are big abundance changes that cause big opacity changes. Some users may wish to make a $\tau_{500\,\mathrm{nm}}$ or $\tau_{1000\,\mathrm{nm}}$ or τ_{whatever} version of ATLAS12.

Some of the equation of state routines date from the 1960s. If there were not good laboratory data for the energy levels, the partition functions generated then were wrong and the ionization potentials were uncertain, especially for the heavier elements, and they are still wrong. The molecules need a separate partition function for each isotopomer. I planned, and still plan, to write a new equation of state routine that uses partition function tables for each species including each isotopomer. Whenever I compute a new line list I automatically generate the energy levels and the partition function. When I computed an iron group line list (Kurucz 1988a), I generated a partition function table for each species. Those are stored in the file PFIRON. I am computing or recomputing all the atoms to fill out the line data so I will generate all the partitiion functions and the problem will be solved. However those calculations are going slowly, especially since I do not have funding. I have decided to try to do a quick Hartree-Fock calculation of the energy levels and the partition functions so that I can finish ATLAS12. Now that memory is not a problem, putting in the new partition functions and depth-dependent abundances should be simple.

The 30 000 fluxes that ATLAS12 computes are accurate enough to compute the total flux but not good enough for intermediate band photometry such as *uvby*. It is necessary to make a separate flux calculation using SYNTHE after a model is converged. I use the following procedure:

I first run ATLAS12 only through the point where it selects the line data from the line list files. I write out and save the file. That file is in a packed format where all information not essential to the opacity calculation has been removed. The lines for any similar stars will be the same, so models for those stars can be computed from the same line list. Models with lower abundances will also work. Higher abundance models would need a new line selection.

To compute the spectrum for an ATLAS12 model with SYNTHE, use program RPACKEDLINE to read the line file. Since there are no identifications in the packed file, SYNTHE does not save any information about the lines. ATLAS9, or any other models, can be used with these line lists. A complete spectrum may have to be

computed in pieces and patched together with MERGESYN. The packed line list can also be edited for computing shorter intervals for photomtery, etc.

These spectra do not reproduce real high resolution observed spectra. Stronger lines tend to have good data but the weaker lines are incomplete and they include the predicted lines with uncertain wavelengths that fill in the opacity between big lines. At lower resolution most of the wavelength errors should average out. Also models are generally computed with an overestimate of the Fe abundance and an overestimate of the microturbulent velocity to make up for some of the missing line opacity.

To make a detailed comparison to a high resolution spectrum, only the line lists with laboratory wavelengths should be used, and the *gf* values and damping constants need to be hand adjusted to match. The normal procedure is to work differentially by adjusting the line data to match a high resolution, high-signal-to-noise atlas for a star for which a good model atmosphere is available.

3.2 Depth-Dependent Microturbulent Velocity

Microturbulent velocity is a parameter that is generally not considered physically except in the sun. Usually it is treated as the parameter that minimizes scatter among lines of the same ion in abundance analyses. Figure 5 shows the temperature *versus* optical depth for the empirical solar Model C of Fontenla *et al.* (1993). It also shows the empirical microturbulent velocity *versus* optical depth determined from (central intensity) line profiles. I have schematically divided it into microturbulent velocity that is produced by convective motions that must go to zero at or below the temperature minimum, and into microturbulent velocity that is produced by the waves that heat the chromosphere. The minimum $V_{\rm turb}$ is about 0.28 of the maximum $V_{\rm turb}$. The minimum temperature is about 0.76 $T_{\rm eff}$. I suggest that all "normally" convective cool stars have behavior like this.

This convective microturbulent velocity is not the microturbulent velocity found in equivalent width abundance analyses. In the sun an equivalent width determination of microturbulent velocity from the flux spectrum yields $V_{\rm turb} < 1$ km s^{-1}. It is also not the $V_{\rm turb}$ of line opacity tables. My solar model, ASUN, (Kurucz 1992) has $V_{\rm turb} = 1.5$ km s^{-1} in order to make up for missing lines that have not yet been included in the line list. We know for certain that the microturbulent velocity varies with depth, that the opacity is strongly dependent on microturbulent velocity, and that the model atmospheres do not include depth-dependent microturbulent velocity.

In Figure 6 I show the maximum convective velocity for a grid of solar abundance convective models. In Figure 7 I show the maximum fraction of convective flux at any depth for each model in Figure 6. In Figure 8 I have weighted the maximum convective velocity by the maximum convective fraction. I treat this weighted velocity $V_{\rm W}$ as the microturbulent velocity at the bottom of the atmosphere. It agrees with the empirical value in the sun. Then I take the depth dependence of the microturbulent velocity produced by convection in the sun and I scale to $V_{\rm W}$. I ignore outwardly increasing $V_{\rm turb}$ from waves and set the minimum

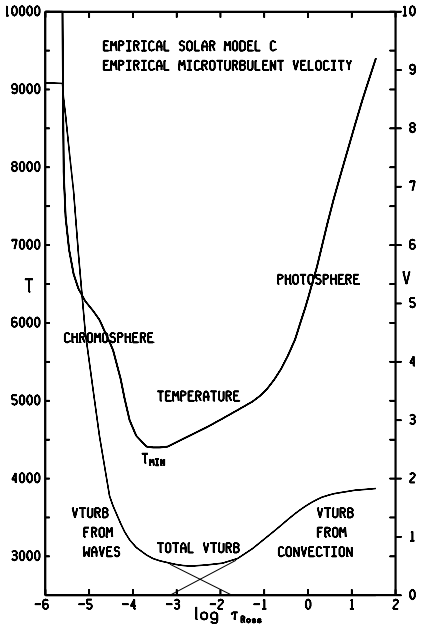

Fig. 5. The empirical solar model C by Fontenla *et al.* (1993) that has a chromosphere, a temperature minimum, and also an empirical microturbulent velocity distribution that I have divided into $V_{\rm turb}$ from convection and $V_{\rm turb}$ from waves.

$V_{\rm turb}$ to max($V_{\rm turb}$, 0.28 $V_{\rm W}$) as in the sun. Figure 8 then gives the variation of microturbulent velocity with temperature and gravity as long as we stay on the cool side of the maximum. And, since we do not understand what is happening on the hot side, let us blindly do the same there. One thing we know for certain is that there can be no microturbulent velocity produced by convective motions if there is no convection. Convection deeper in the star can generate waves that propagate through the atmosphere and produce a "wave" $V_{\rm turb}$. One can also guess that the "mean" microturbulent velocity must be on the order of $V_{\rm W}/2$ which should roughly correspond to the number found from curves of growth.

Microturbulent velocity varies with effective temperature and gravity and abundance because convection varies with effective temperature, gravity, and abundance. When comparing the properties of two stars, the difference in microturbulent velocity must be accounted for. When comparing two stages along an evolutionary track, the change in microturbulent velocity must be accounted for. By using grids with depth-dependent microturbulent velocity as described here, this effect is automatically included. $V_{\rm turb}$ is no longer a free parameter. This may not be true for low-gravity stars hotter than the sun that have only weak convection.

If two stars have the same effective temperature and gravity, the one with the higher abundances will have higher microturbulent velocity because it is more

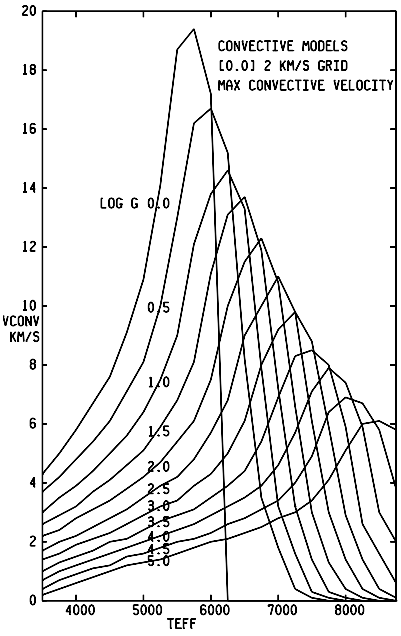

Fig. 6. Maximum convective velocity at any depth in each model for a solar abundance grid.

convective. I have not yet computed the grids to work out the numbers. I expect that in ATLAS12 the $V_{\rm turb}$ varies with the convection, the convection varies with the Rosseland opacity at $\tau = 1$, and the Rosseland opacity at $\tau = 1$ varies with the abundances.

3.3 Rotation and Differential Rotation

Rotational broadening is computed in program ROTATE by generating intensity spectra for a range of angles (currently 17, μ = 1.0, .9, .8, .7, .6, .5, .4, .3, .25, .2, .15, .125, .1, .075, .05, .025, .01), then defining a rectilinear grid over the disk of the star (currently 200×200, or 100×100 quadrant), then interpolating the spectrum for the angle and projected velocity at each point, and finally summing all the points. There are two more approximations. First the spectra are interpolated to 100 angles (μ = 0.005 to 0.995 by .010) and pretabulated. The spectrum at each point on the disk is found by choosing the nearest angle in the pretabulation. Second, the spectrum is doppler shifted by the nearest integral number of points. If the resolving power is 500 000 the shift can have an error of one part in one million. Most of the errors are random and cancel but they should be checked for critical work. Increase the resolving power or the grid size or the number of angles and see if the output spectrum is affected.

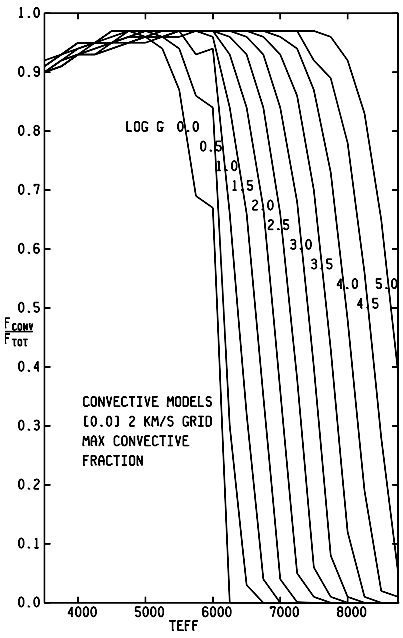

Fig. 7. Maximum fraction of convective flux at any depth in each model for a solar abundance grid.

More physics can be put in. I have added differential rotation using the empirical fit for the sun from Libbrecht and Morrow 1991 for latitude ϕ and $R_\odot$ in km,

$V_{\rm rot}(\phi) =$

$(462 - 75\sin^2\phi - 50\sin^4\phi)10^{-9}\ 2\pi R_\odot,$

$V_{\rm rot}(0) = 2.020\ {\rm km\,s^{-1}}$ at the equator,

$V_{\rm rot}(1) = 1.474\ {\rm km\,s^{-1}}$ at the pole,

$V_{\rm rot}(\phi)/V_{\rm rot}(0) =$

$(1\ -75/462\sin^2\phi\ -50/462\sin^4\phi).$

The parameter read by ROTATE is the stellar equitorial velocity. Differential rotation is assumed to have the same behavior for all stars. It is computed only if it is explicitly turned on.

As long as physical variables can be defined on an array of points and there is a procedure for interpolating in a grid of spectra that vary in those physical variables, one can treat any shape star, or binaries, spots, rapid rotators, etc. using similar methods.

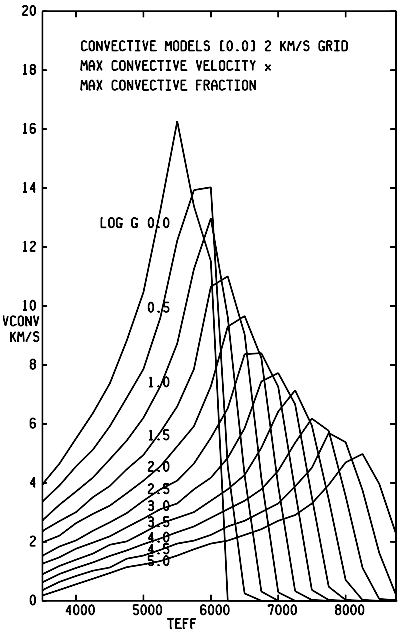

Fig. 8. The product of Figure 2 times Figure 3, the flux-weighted convective velocity, which I use as the estimator of $V_{\rm turb}$ at the bottom of a model.

3.4 Atmospheric Transmission

In 1988 I discovered (Kurucz 1988b) that there were broad features in Kitt Peak FTS solar spectra (taken by James Brault) that were produced by ozone and by $[O_2]_2$ (O_2 dimer) that I had not known about and had not considered in the reduction of the Solar Flux Atlas (Kurucz *et al.* 1984). The $[O_2]_2$ number density is quadratic in O_2 so is concentrated near the ground. It produces strong features at sunset and sunrise. Figures 9–11 show the features produced by O_3, $[O_2]_2$, and their product in the visible. There are also many lines of O_2 and H_2O that blend with, or that mask, solar lines in the FTS spectra shown in Figure 12.

Much of the research on atmospheric transmission has been done by the United States Air Force (Air Force Research Laboratory, formerly Air Force Geophysics Laboratory, formerly Air Force Cambridge Research Laboratory). They have produced empirical model atmospheres, line data (HITRAN), and computer programs for calculating transfer through the atmosphere (LOWTRAN, MODTRAN). These programs are not designed for doing the whole spectrum at once in high resolution.

Astronomers should measure the atmosphere over their heads and determine the run of temperature, pressure, O_3, and H_2O with altitude because it affects their observations, but they do not care. The Air Force had a program of measuring these quantities and has produced averaged models for the whole year, or quarterly, or monthly, for temperate latitudes, tropical latitudes, etc. (Anderson *et al.* 1986).

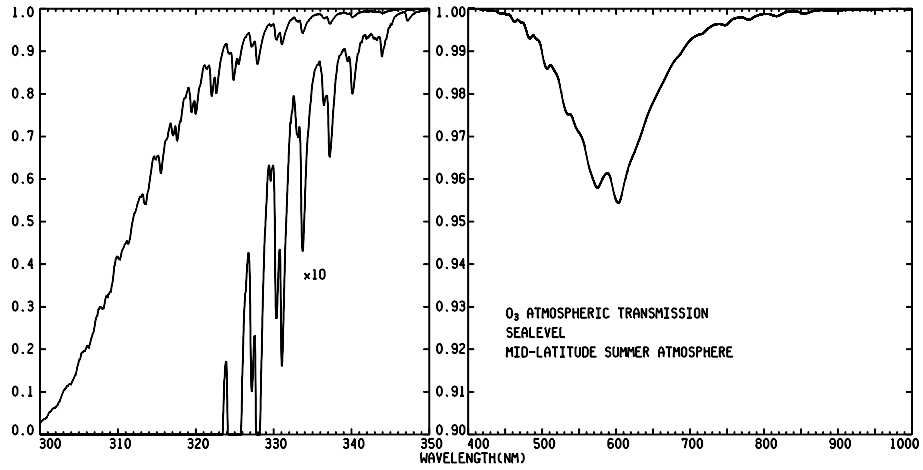

Fig. 9. Telluric O_3 transmission from 300 to 1000 nm.

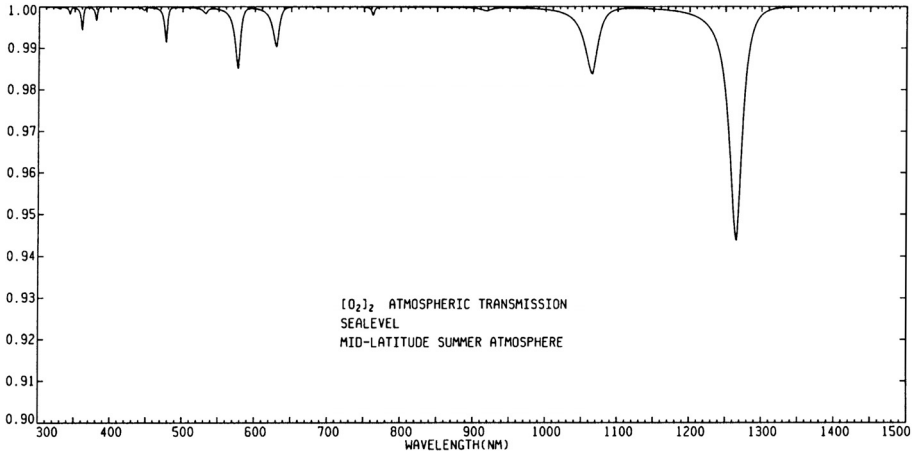

Fig. 10. Telluric $[O_2]_2$ transmission from 300 to 1500 nm.

From those models I have made up four models MODMIDWIN, MODSPRING, MODMIDSUM, and MODAUTUMN that I use to represent the atmosphere above Kitt Peak. They can be used as starting guesses at any observatory except in Antarctica. The temperatures, pressures, O_3, and H_2O, must be adjusted to get a good fit for any observed spectrum. MODMIDSUM is listed in Table 2.

Laboratory ozone cross-sections for the ultraviolet Hartley & Huggins (Bass & Paur 1981; Griggs 1968; Freeman *et al.* 1983) and the visible Chappuis & Wulf (tabulated by Shettle & Anderson 1995) bands are tabulated for several temperatures and interpolated. Widths and strengths of individual O_2 dimer

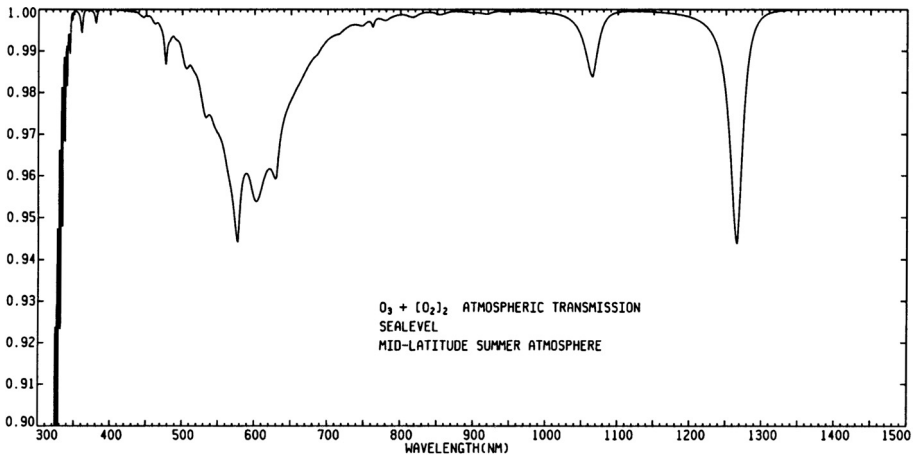

Fig. 11. Telluric O_3 and $[O_2]_2$ transmission from 300 to 1500 nm.

[Fig. 12 is a large color ledger page on the Kurucz website `KURUCZ.HARVARD.EDU/PAPERS/TRANSMISSION/FIG5`. It will be mailed by post on request.]

Fig. 12. Telluric lines of O_2 and H_2O that were computed for the flux scans in the Kitt Peak Solar Flux Atlas (Kurucz 2005) and pieced together in the solar laboratory frame with gravitational red shift removed.

features have been measured in the laboratory (Greenblatt *et al.* 1990; Dianov-Klokov 1959) and computed from those parameters.

The main source of line data is the HITRAN (HIgh-resolution TRANsmission) database (Rothman *et al.* 2005). Smithsonian Astrophysical Observatory has taken over management of the database from the Air Force. Historically the Air Force concentrated on infrared data beyond 1 μm aiming for very accurate line positions, strengths, pressure-shifts, and damping constants. Researchers all over the world work on and with HITRAN, not just the Air Force. The visible data were poor quality. Much of it was missing or wrong. Now about half of the O_2 and H_2O are good. I have tried to fill in missing lines for O_2 by calculating them and by fitting them in solar spectra. There are calculations available for H_2O but they do not work very well. I have tried to adjust many of the lines by hand. One of the main problems with these lines, one that astronomers have not yet had to face, except in Stark broadening, is pressure shifts. The measured positions of telluric lines in the solar spectra are not the real line positions. If they are used to generate molecular constants, they introduce systematic errors. Laboratory work is required to measure the line positions as a function of pressure and to extrapolate to zero pressure. Only the strongest bands of O_2 have been well measured.

Table 2. Mid-Latitude summer (July) atmosphere.
after Anderson et al. (1985)

H(km)	P(Mb)	T(K)	Ntot(/cm3)	H2O(ppmv)	O3(ppmv)
0.	1013.	294.2	2.496E+19	1.88E+04	3.02E-02
1.	902.	289.7	2.257E+19	1.38E+04	3.34E-02
2.	802.	285.2	2.038E+19	9.68E+03	3.69E-02
3.	710.	279.2	1.843E+19	5.98E+03	4.22E-02
4.	628.	273.2	1.666E+19	3.81E+03	4.82E-02
5.	554.	267.2	1.503E+19	2.23E+03	5.51E-02
6.	487.	261.2	1.351E+19	1.51E+03	6.41E-02
7.	426.	254.7	1.212E+19	1.02E+03	7.76E-02
8.	372.	248.2	1.086E+19	6.46E+02	9.13E-02
9.	324.	241.7	9.716E+18	4.13E+02	1.11E-01
10.	281.	235.3	8.656E+18	2.47E+02	1.30E-01
11.	243.	228.8	7.698E+18	9.56E+01	1.79E-01
12.	209.	222.3	6.814E+18	2.94E+01	2.23E-01
13.	179.	215.8	6.012E+18	8.00E+00	3.00E-01
14.	153.	215.7	5.141E+18	5.00E+00	4.40E-01
15.	130.	215.7	4.368E+18	3.40E+00	5.00E-01
16.	111.	215.7	3.730E+18	3.30E+00	6.00E-01
17.	95.0	215.7	3.192E+18	3.20E+00	7.00E-01
18.	81.2	216.8	2.715E+18	3.15E+00	1.00E+00
19.	69.5	217.9	2.312E+18	3.20E+00	1.50E+00
20.	59.5	219.2	1.967E+18	3.30E+00	2.00E+00
21.	51.0	220.4	1.677E+18	3.45E+00	2.40E+00
22.	43.7	221.6	1.429E+18	3.60E+00	2.90E+00
23.	37.6	222.8	1.223E+18	3.85E+00	3.40E+00
24.	32.2	223.9	1.042E+18	4.00E+00	4.00E+00
25.	27.7	225.1	8.919E+17	4.20E+00	4.80E+00
27.5	19.07	228.5	6.050E+17	4.45E+00	6.00E+00
30.	13.2	233.7	4.094E+17	4.70E+00	7.00E+00
32.5	9.30	239.0	2.820E+17	4.85E+00	8.10E+00
35.	6.52	245.2	1.927E+17	4.95E+00	8.90E+00
37.5	4.64	251.3	1.338E+17	5.00E+00	8.70E+00
40.	3.33	257.5	9.373E+16	5.10E+00	7.55E+00
42.5	2.41	263.7	6.624E+16	5.30E+00	5.90E+00
45.	1.76	269.9	4.726E+16	5.45E+00	4.50E+00
47.5	1.29	275.2	3.390E+16	5.50E+00	3.50E+00
50.	.951	275.7	2.500E+16	5.50E+00	2.80E+00
55.	.515	269.3	1.386E+16	5.35E+00	1.80E+00
60.	.272	257.1	7.668E+15	5.00E+00	1.30E+00
65.	.139	240.1	4.196E+15	4.40E+00	8.00E-01
70.	.0671	218.1	2.227E+15	3.70E+00	4.00E-01
75.	.0300	196.1	1.109E+15	2.95E+00	1.90E-01
80.	.0120	174.1	4.996E+14	2.10E+00	2.00E-01
85.	.00448	165.1	1.967E+14	1.33E+00	5.70E-01
90.	.00164	165.0	7.204E+13	8.50E-01	7.50E-01
95.	.000625	178.3	2.541E+13	5.40E-01	7.00E-01
100.	.000258	190.5	9.816E+12	4.00E-01	4.00E-01

I have written subroutines OZONE and O2DIMER for computing the transmission spectra of the broad features and the TRANSYNTHE suite of programs for treating telluric lines. The cause of the delay, as for solar lines, is that the telluric data are still not good enough to treat the problem without hand adjustment, even for O_2, and there are many missing lines.

Files AIR1, AIR2, AIR3, ..., AIR10, AIR20, AIR100, AIREND have telluric line data for 0 to 1 μm, 1 to 2 μm, etc. Most of the data except in AIR1 are from HITRAN reformatted like other data in the Kurucz linelists. Some of the data have hand corrections. The overall quality at short wavelengths is not good. Every line should be checked for critical work.

TRANSYNBEG reads the input parameters. The wavelength range and resolution must be the same as in any subsequent stellar spectrum calculation. The lines are shifted by the radial velocity of the star which must be specified. In wavelength regions where sharp telluric lines are present, the resolving power of the calculation must be at least 2 million to treat the sub-300 K doppler width. Any computed stellar spectra must have the same resolution.

RMOLAIR reads the line data from the AIR* files.

TRANSYNTHE computes the opacity spectrum.

TRANSPECTR computes the mean transmission spectrum from the given starting and stopping airmass, starting and stopping hour angle, mean declination, latitude, and altitude. It also computes the residual depth of each line. The line data and depth are passed along with the spectrum for labelling plots.

TRANSMIT multiplies a stellar spectrum by the transmission spectrum.

3.5 Spectrophotometry

Once the computed spectrum has been computationally transmitted from the star to the instrument it is instrumentally broadened for comparison to observation. Program BROADEN convolves a Gaussian, $\sin(x)/x$, or rectangular profile specified by FWHM in velocity, wavelength, wavenumber, or resolving power. It also can use instrumental profiles specified at the computed point spacing. When the profile is rapidly changing, program BROADENX linearly interpolates between profiles specified at the ends of a wavelength interval.

Now, when I compute a model that I think might be of general interest, I compute the spectrum as far to the ultraviolet and infrared as I can. Then I broaden it to resolving powers of 500 000, 100 000, 50 000, 30 000, 20 000, 10 000, 5000, 3000, 2000, 1000, 500, 300, 200, and 100 and put those spectra on my website in the STARS directory so people can find predictions"off the shelf" to compare to their observations. It takes about one day per model.

3.6 Photometry

Photometry is computed by convolving the spectra output from the SYNTHE suite of programs with a theoretical model of the observation. That model would include detector response, filter transmission, transmission of the obtical system, and, for an observation from the ground, transmission of the atmosphere. I have written a simple program INTEGRATEFILTER that convolves SYNTHE output spectrum with a response function in this way. INTEGRATEFILTER will read any number of response functions. The Asiago Database (Moro & Munari 2000) has the most photometric systems so I suggest that some user make up a general input file from it and a program to generate all the colors.

The atmospheric transmission is computed with the TRANSYNTHE suite of programs and is applied to the spectra before INTEGRATEFILTER is used. Most filter systems in the visible and near infrared are insensitive to the atmospheric transmission, while ultraviolet and infrared systems are sensitive.

3.7 Limbdarkening

Limbdarkening is automatically produced when I generate a spectrum for a rotating star but the files are so big that I have been throwing them away. The rotation program computes the intensity spectrum at a number of angles across the disk (currently 17 angles) and interpolates the spectrum at each point on a rectangular mesh overlaid on the disk. Those spectra are tabulated at all the angles for each wavelength. If the file is transposed to all the wavelengths at each angle, limbdarkening is computed by convolving those spectra with a theoretical model of the observation. That model would include detector response, filter transmission, transmission of the obtical system, and, for an observation from the ground, transmission of the atmosphere. I have written simple programs SPLIT17SYN and INTEGRATEFILTER that convolve a SYNTHE output spectrum with a response function in this way. INTEGRATEFILTER will read any number of reponse functions. The atmospheric transmission is computed with the TRANSYNTHE suite of programs and is applied to the intensity spectra before INTEGRATEFILTER is used. Most filter systems in the visible and near infrared are insensitive to the atmospheric transmission.

3.8 PLOTSYN

I make large plots that compare computed and observed spectra and that actually show errors and provide information to the reader. The features are labelled and the wavelengths and energy levels can actually be read off the plots, and there is a file giving complete information for each labelled line. In addition there is a hand-editable file that gives the input data for evey line that contributed to the spectrum. That file can be read back in to iterate on the fit.

My plotting software was written before Postscript was invented. At present PLOTSYN writes a binary vector file that must be translated to Postscript. I am going to rewrite the plotting utilities, PLOTPACK, to write Postscript directly. (It is simple.) This will make the files smaller, scalable, and editable. I am considering ways to put plots on CDs or DVDs. Perhaps solar spectra at 1 Å per page with line identifications to be used as a reference, or big continuous plots that can be windowed.

4 New Atlases for Solar Flux, Irradiance, Central Intensity, and Limb Intensity

The low resolution, low-signal-to-noise spectra that astronomers normally work with do not contain enough information, in themselves, for interpretation. Without *a priori* knowledge of the atomic and molecular line data for each significant line in the blended features any inferences about abundances have large uncertainties. Reliable atomic and molecular data are not available from the laboratory or from theory except for a small fraction of the lines. Atlases of high-resolution, high signal-to-noise spectra of stars with low projected rotation velocity provide

information about details and blending in the spectra. People who work with stellar spectra should always check their wavelength region in high quality atlases. If the atlas was taken from the ground, it will also show the telluric lines and their contribution to blends.

I have been trying to make atlases with line identifications for the sun for 25 yeers so that I could check my calculated spectra against reality. When I can find patterns in the errors, I try to correct the physics. However, the calculated spectra have been so poor that almost every line needs to be adjusted to match the observed spectra. Many of the lines in the observed spectra are missing altogether from the line list. The calculations are also needed for the reduction of the observed spectra themselves because the continuum placement depends on many weak blends and on the damping treatment of the wings of many lines.

Matching observed spectra seems to be hopeless, at least in the near future. I have finally decided that the continuum placement is good enough, and that I should publish the spectra with only "suggestive" calculations and identifications to give the user an idea of where to begin and what the problems are.

4.1 New Atlases

I have fifty solar FTS scans taken by James Brault and Larry Testerman at Kitt Peak. The scans cover the central intensity, limb ($\mu = 0.2$), and flux spectrum from 0.3 to 5.5 μm. The central intensity for 1.0 to 5.5 μm was published by Delbuille *et al.* (1981). The flux spectrum from 0.3 to 1.3 μm was published as Solar Flux Atlas (Kurucz *et al.* 1984. However, since then I have learned that broad O_3 and O_2 dimer (or $[O_2]_2$) features are present in the spectrum, and I have improved the line data and the continuum treatment. I have produced an improved version of the flux atlas (Kurucz 2005a) that is available on my web site KURUCZ.HARVARD.EDU. I have merged the scans into a single spectrum, but I also present each scan separately because each FTS scan has its own atmospheric model, air mass, telluric spectrum, and radial velocity. The resolving power and signal-to-noise vary from scan to scan and are on the order of 300 000 and 3000 respectively. I am now working on similar atlases for central intensity and limb spectra. If I get funding, I will continue the atlases into the infrared to 5.5 μm. I will produce atlases plotted at one Å/page that include the computed spectrum and line identifications. If I can get funding, I will distribute paper and DVD copies.

The telluric line spectrum was computed using HITRAN (Rothman *et al.* 2005) and other line data for H_2O, O_2, and CO_2. The line parameters were adjusted for an approximate match to the observed spectra. I was able, through many hand adjustments, to remove the telluric absorption spectrum for the flux atlas and to recover the residual irradiance spectrum above the atmosphere for the region from 0.3 to 1.0 μm. Figure captions 1 to 13 outline the reduction procedure. In wavelength regions with heavy absorption the quality has been compromised by more than an order of magnitude. I have produced a continuous atlas of this

irradiance spectrum (Kurucz 2005b). Most of the irradiance atlas has the same resolution and signal-to-noise as the flux atlas.

Given a calculated or semiempirical solar model, the continuum level can be computed and multiplied by the residual irradiance spectrum to produce the absolute irradiance spectrum at high resolution. Alternatively, the high resolution residual irradiance spectrum can be broadened and smoothed to match the resolution of any low resolution irradiance spectrum and normalized to the low resolution spectrum. That normalization can be applied to the high resolution spectrum to obtain a high resolution absolute irradiance spectrum. An example for each method is presented below. This is the spectrum that illuminates the Earth and all other bodies in the solar system. This is a typical G star spectrum like those that illuminate extra-solar planets.

4.2 Figure Captions for Irradiance Atlas

The figures are in color, are ledger size, and are too large for this volume. The figures and a table of the observations are on my web site `KURUCZ.HARVARD.EDU/PAPERS/TRANSMISSION`. They are large files. I will send paper copies of a poster on the irradiance atlas (Kurucz 2005c) by post on request. The figure captions, in themselves, provide an explanation of the reduction procedure.

Table 1. Record of the observations.

Fig. 1. The old Kitt Peak Solar Flux Atlas. There are eight overlapping FTS scans that were normalized and pieced together to form a continuous residual spectrum. The observational data for the scans is listed in Table 1. (There are only seven scans in this figure because the eigth is beyond 1000 nm.) The next figures show the re-reduction of these scans.

Fig. 2. Broad atmospheric features of O_3 and $[O_2]_2$ that were present in the scans but not considered. Each scan was assigned to an atmospheric model listed in Table 2. The O_3 and $[O_2]_2$ transmission was computed using programs available on my website, `kurucz.harvard.edu`, and divided out. (The transmissions for the seven scans were pieced together for the plot.)

Fig. 3. The blue end of one of the FTS scans is shown in green. A continuum, smooth green line, is subjectively fitted to the scans by comparing to predictions from calculations of the solar spectrum and the telluric spectrum. When a reasonable looking fit has been obtained through iteration, the spectrum is divided by the continuum value to produce a residual spectrum shown in red. The top 1 percent of the residual spectrum is replotted in red as well. The blue curve is the the transmission curve for O_3 and $[O_2]_2$ that has already been divided out.

In **Fig. 4.** the scans were blueshifted to remove the gravitational red shift and pieced together in the solar laboratory frame in air. This is the revised spectrum of the Kitt Peak Solar Flux Atlas.

Fig. 5. Telluric lines of O_2 and H_2O that were computed from the atmospheric model for each scan in the solar laboratory frame with gravitational red shift removed. (The seven scans are pieced together.)

Fig. 6. A sample calculation of the spectrum for a relatively empty angstrom at 599.1 nm in the Solar Flux Atlas shown in Figure 4. The telluric, solar, and observed spectra are labelled at normal scale and 10 times scale.
Fig. 7. shows the irradiance spectrum obtained from the spectra in Figure 6 by dividing out the telluric spectrum. For stronger telluric lines and lines with incorrect wavelengths, there are artifacts that appear in the irradiance spectrum that were removed by hand and replaced with a linear interpolation.
Fig. 8. The residual irradiance spectrum after all the scans have been processed and pieced together in the solar laboratory frame in vacuum with gravitational red shift included.
Fig. 9. The predicted level of the continuum for theoretical solar model ASUN (Kurucz 1992).
Fig. 10. The absolute irradiance spectrum obtained by normalizing the residual irradiance spectrum shown in Figure 8 to the continuum level shown in Figure 9.
Fig. 11. The reference irradiance spectrum proposed by Thuillier *et al.* (2004).
Fig. 12. The Kitt Peak absolute irradiance spectrum smoothed using a 0.5 nm triangular bandpass that approximates the resolution of Thuillier *et al.* and then compares the two spectra. Note the probable overestimation of the ozone below 320 nm and around 600 nm in the Kitt Peak atlas. (Remember that ozone has been divided out.) I will probably have to re-reduce those scans. Note the flux discrepency in the G band. It appears that model ASUN does not produce enough flux, perhaps becase of insufficient opacity below 300 nm that results in too low a temperature gradient. I am adding more line opacity. I will try to produce a better model. Of course, there may also be errors in Thuillier *et al.* as well.
Fig. 13. The Kitt Peak irradiance spectrum subjectively normalized to the Thuillier *et al.* irradiance spectrum. I recommend this spectrum as the high resolution irradiance spectrum. The procedure for removing telluric lines introduces noise into the irradiance spectrum where there were telluric lines. The flux atlas itself should be used for abundance analysis or other critical work.

References

Anderson, G.P., *et al.*, 1986, AFGL-TR-86-0110

Bass, A.M., & Paur, R.J., 1981, J. Photochem. 17, 141

Castelli, F., & Kurucz, R.L., 1993, in Modelling of Stellar Atmospheres, N. Piskunov, W.W. Weiss, & D.F. Gray eds., IAU Symp., 210, A20

Cowan, R.D., 1968, JOSA, 58, 808

Delbouille, L., Roland, G., Brault, J., & Testerman, L., 1981, Photometric Atlas of the Solar Spectrum from 1850 to 10 000 cm^{-1}, Kitt Peak National Observatory (Tucson), 189

Dianov-Klokov, V.I., 1959, Opt. Spectrosc., 6, 290

Fontenla, J., Avrett, E.H., & Loeser, R., 1993, ApJ, 406, 310

Freeman, D.E., *et al.*, 1983, P&SS, 32, 239

Greenblatt, G.D., *et al.*, 1990, JGR, 95D, 18577

Grevesse, N., & Sauval, A.J., 1999, A&A, 347, 348

Griggs, M., 1968, JCP, 49, 857

Herbig, G.H., 1995, ARA&A, 33, 19

Johansson, S., 1978, Phys. Scr., 18, 217

Kurucz, R.L., 1988a, in Trans. IAU XXB. M. McNally ed. (Dordrecht: Kluwer), 168

Kurucz, R.L., 1988b, in Infrared Extinction and Standardization, E. Milone ed. (Berlin: Springer-Verlag), 55

Kurucz, R.L., 1992, in Stellar Population of Galaxies, B. Barbuy & A. Renzini eds. (Dordrecht: Kluwer), 225

Kurucz, R.L., 1995, in Stellar Surface Structure, K.G. Strassmeier & J.L.Linsky ed. (Dordrecht: Kluwer), 523

Kurucz, R.L., 2002, in Atomic and Molecular Data and their Applications. D.R. Schultz, P.S. Krstic & F. Ownby ed., AIP Conf. Proc., 636, 134

Kurucz. R.L., 2005a, Kitt Peak Solar Flux Atlas 300 to 1000 nm, in preparation

Kurucz, R.L., 2005b, Kitt Peak Irradiance Atlas 300 to 1000 nm, in preparation

Kurucz, R.L., 2005c, High resolution irradiance spectrum from 300 to 1000 nm presented at AFRL Transmission Meeting, 15–16 June 2005, Lexington, Mass

Kurucz, R.L., & Avrett, E.H., 1981, Solar spectrum synthesis. I. A sample atlas from 224 to 300 nm, SAO Spec. Rep., 391, 139

Kurucz, R.L., Furenlid, I., Brault, J., & Testerman. L., 1984, Solar Flux Atlas from 296 to 1300 nm. National Solar Obs., Sunspot, New Mexico., 240

Langhoff, S.R., 1997, ApJ, 481, 1007

Libbrecht, K.G., & Morrow, C.A., 1991, in The Solar Interior and Atmosphere, A.N. Cox, W.C. Livingston, & M. Matthews eds. (Tucson: University of Arizona Press), 479

Litzén, U., Brault, J.W., & Thorne, A.P., 1993, Phys. Scr., 47, 628

Marcy, G.W., & Butler, R.P., 1992, PASP, 104, 270

Moro, D., & Munari, U., 2000, A&AS, 147, 361

Osterbrock, *et al.*, 2000, PASP, 112, 733

Partridge, H., & Schwenke, D.W., 1997, J. Chem. Phys., 106, 4618

Pickering, J.C., 1996, ApJS, 107, 811

Pickering, J.C., & Thorne, A.P., 1996, ApJS, 107, 761

Rosberg, M., Litzén, U., & Johansson, S., 1993, MNRAS, 262, L1-L5

Rothman, L.S., *et al.*, 2005, JQSRT, 96, 139

Schwenke, D.W., 1998, Faraday Discussions, 109, 321

Shettle, E.P., & Anderson, S.M., 1995, PL-TR-95-2060

Slanger, T.G., *et al.*, 2003, PASP, 115, 869

Sugar, J., & Corliss, C., 1985, J. Phys. Chem. Ref. Data, 14, Supp. 2

Thuillier, G., Floyd, L., Woods, T.N., *et al.*, 2004, in Solar Variability and its Effect on the Earth's Atmosphere and Climate System, J.M. Pap *et al.* eds., AGU, Washington, DC, p. 171

Tsymbal, V., & Shulyak, D., 1993, in Modelling of Stellar Atmospheres, N. Piskunov, W.W. Weiss, & D.F. Gray, eds., IAU Symp., 210, A15

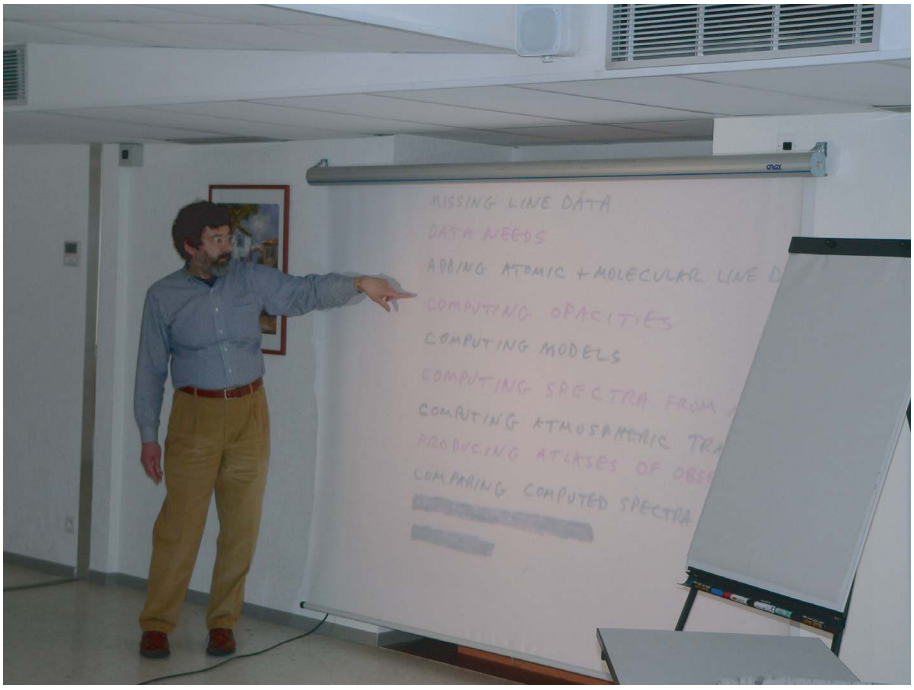
MISSING LINE DATA
DATA NEEDS
ADDING ATOMIC + MOLECULAR LINE
COMPUTING OPACITIES
COMPUTING MODELS
COMPUTING SPECTRA FROM
COMPUTING ATMOSPHERIC
PRODUCING ATLASES OF
COMPARING COMPUTED SPECTRA